2010 NDIA GROUND VEHICLE SYSTEMS ENGINEERING AND TECHNOLOGY SYMPOSIUM
MODELING & SIMULATION, TESTING AND VALIDATION (MSTV) MINI-SYMPOSIUM
AUGUST 17-19 DEARBORN, MICHIGAN

# A HYBRID IMPULSIVE SCHEME FOR FASTER THAN REAL-TIME VEHICLE LOADS PREDICTION

**James Critchley, PhD**
BAE Systems
U.S. Combat Systems
Troy, MI

**Paramsothy Jayakumar, PhD**
U.S. Army
RDECOM-TARDEC
Warren, MI

## ABSTRACT

*Faster than real-time and real-time vehicle dynamic models run with fixed time step integrators, without accuracy control and usually apply numerous approximations to obtain a stable solution. These models generally provide very good descriptions of the system behavior, capturing the gross motions and character of the response. However, the consequence of approximation and the lack of error control is that the resulting loads cannot be trusted for structural design analysis. Nonetheless, these lightweight faster than real-time models are indispensible in concept development where an unlimited number of designs may be considered in the automated exploration of the design space. This work investigates a novel simulation technique in an attempt to converting the family of real-time vehicle dynamics models into reliable first order structural load predictors. The method applies an error estimator to the real-time fixed step integrator to identify loss of accuracy in stiff models with resolution to the offending degree(s) of freedom. Inaccurate and potentially unstable time steps are then replaced by an impulse-based solution and the time-step recomputed. The required impulsive load can then be transformed (on or off-line) into a repeatable and accurate load pseudo-time history through integration of an independent nonlinear contact event. A simple tracked vehicle model example is used to demonstrate the features of the solution which is validated by comparison to results obtained from fully integrated trajectories.*

## INTRODUCTION

Vehicle loads prediction in off-road and durability environments runs significantly slower than real-time. The computationally intensive nature of these simulations is attributed to stiff nonlinearities which must be resolved to provide accurate forcing profiles. In contrast, vehicle performance simulations frequently run faster than real-time and are able to ignore stiff contributions via exact joint constraints, state limits, truncated stiffness, and fixed time step explicit integrators (no error control). Put simply, the objective of a real-time model is to run in a stable manner through extreme events and the resulting loads are virtually meaningless. Nonetheless, these lightweight faster than real-time models are indispensible in concept development where an unlimited number of designs may be considered in the automated exploration of the design space.

Detailed analysis models of ground vehicle systems can be used to accurately predict the loads, handling characteristics, and other performance attributes of vehicles as they are being designed [1]. Such system models rely on detailed component models which reproduce component test data such as is common for tires [2], shock absorbers [3], and springs [4]. When assembled in various configurations, the results can very accurately represent reality but come at a large computational cost.

Real-time vehicle models synchronize simulation results with a wall clock at regular intervals so that data can be exchanged as required for visualization and interactive control. Traditional applications of real-time vehicle models support operator-in-the-loop simulations for training purposes. Historical limitations on computing power necessitated that the first models be limited to gross approximations of six degree of freedom vehicle motion correlated directly to the system response.

Today computing resources are such that in practice only rigid body and exact joint constraints are needed to be applied for routine driving conditions. The application of real-time simulations has similarly expanded to support hardware-in-the-loop simulation and rapid dynamic evaluations as required for design iteration in the concept design phase and virtual verification of handling requirements, all from a single model [5]. However, approximation is still required in the stiffest regions of the response. The jounce and rebound bumpers may be omitted

and replaced by travel limits imposed on the numerical integrator or the simulation may simply be allowed to go unstable after extreme events.

The fixed time step integration routines used in real-time dynamics are required to arrive at an updated system state in a deterministic number of computations and therefore "fixed" amount of time. The extent to which the wall clock time per state update is fixed is highly dependent on the host computer's operating system. But in practice any routine and hardware combination which reliably provides output before it is required by interactive applications is called real-time. The real-time system time step is then determined by the speed and availability of the computing resource. Faster computers can take smaller steps in the same amount of time.

Explicit integration routines are very efficient and commonly used for real-time dynamics. They become unstable for high frequencies because the time derivatives of the states are used to calculate the state update and the shape function applied over the interval can only capture a small amount of curvature or oscillation. Having pre-determined the fixed time step size based on the computing resource, the system model must be altered in stiff regions to maintain uniform stability.

In practice the high frequency contributions which are removed are observed to have no bearing on the gross mobility output of models. In other words, the real-time model simply finds a way "through" any stiff events and does not attempt to reliably model them. To this end, any number of other "cheats" may be applied.

Generally speaking the modeling approximations should not be interpreted as software tool limitations. For multipurpose models, approximations may be applied only when the model is selected when real-time output (fixed step integration) is desired.

The same real-time models can run faster than real-time to assist in vehicle concept evaluations. A critical aspect of vehicle design is durability which in turn requires accurate prediction of loads and associated cycles. The removal of stiff responses and loss of accuracy due to fixed step integration renders real-time models unable to accurately predict the most critical peak loads. To estimate loads the analyst can remove approximations and run with variable step time integration (to assure accuracy). However, this also reintroduces the computational burden associated with detailed analysis. Assessment of virtual vehicles over rough durability courses representing continuous operation in the stiffest regions of the response will not then be suitable for rapid concept iterations in the same way that handling, braking, and other performance predictions can be supported. The value of geometry, weight, and performance target verification in the concept phase is then significantly diminished if the coupled durability performance cannot also be estimated.

A rapid loads model is also an important feature which can be deployed on board vehicles. Applications include optimal suspension control algorithms, condition based maintenance, and intelligent systems task selection. An optimal suspension should act to minimize loads and extend component life. Real-time processing of vehicle motions obtained from minimal and distributed sensors to applied loads allows for condition based replacement of parts and advanced ordering of spares. Intelligent systems require advanced simulation of events to determine appropriate path and speed for mission performance.

The usefulness of rapid vehicle simulations combined with load prediction is many-fold. The following sections describe and apply a new hybrid impulsive modeling technique for loads assessments in this context. First a limited example real-time tracked vehicle model is described and applied to directly demonstrate the issue to be resolved. The nature of fixed and variable step integration is briefly discussed and the example vehicle is simulated to demonstrate the performance of each. The hybrid integration stepping scheme is then outlined and the impulsive assumptions and equations given. The solution is then demonstrated with impulsive forces which may be integrated to reconstruct the loads in a decoupled form. The results are then summarized and future work is discussed.

## A TRACKED VEHICLE EXAMPLE

A minimal tracked vehicle model is introduced for the purpose of demonstrating the relative performance of fixed step and adaptive step integrators. The model need only contain the essential limiting features and as stated earlier the key issue centers on stiffness. The stiffest part of the vehicle response which contributes directly to loads is the "hard" stop at the limits of suspension travel and the ground interactions. From this perspective, many vehicle details can be modeled by simple assumptions (the track in particular) which also allows for a brief and complete description of the vehicle model.

### *Vehicle:*

The ten road wheel tracked vehicle model is depicted in Figure 1. The hull measures roughly 6x2.5x2.5 meters, has a mass of 10,000 kg, and a mass distribution consistent with a uniform solid box of the same dimension about its center of mass (CM). The road arm stations are left/right symmetric with all attachment points 0.5 meters below the CM and laterally offset by 1.25 meters. In the longitudinal direction the offset points are spaced evenly in every 1.5 meters with the center attachment positioned 0.4 meters in front of the CM.

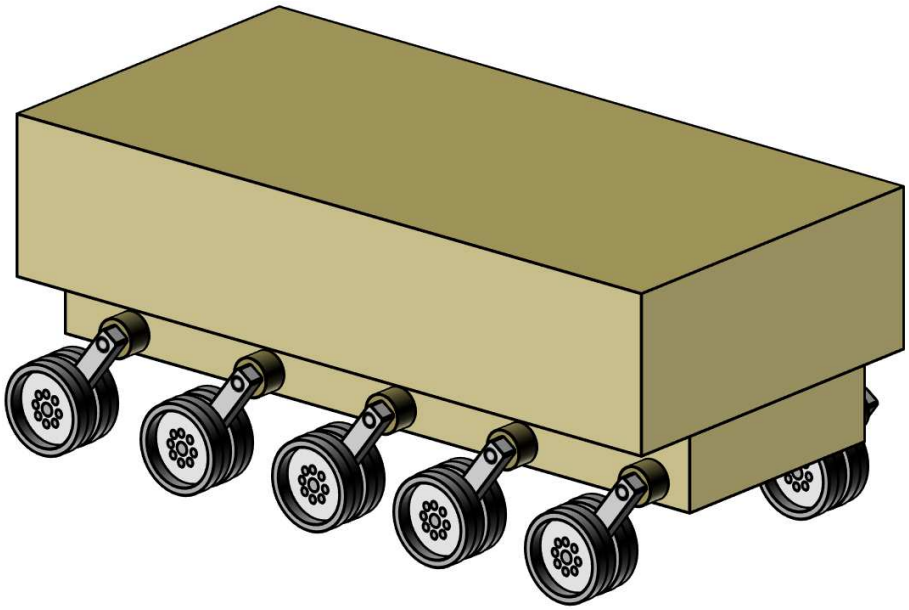

**Figure 1:** Tracked vehicle model.

The hull body is rigid and located in three dimensional space by global *x*,*y*,*z* coordinates corresponding to forward, left, and up and the ordered rotation set, yaw-pitch-roll. The derivatives of these coordinates complete the system state with the exception of the rotation angles which use the derivatives of quasi-coordinates [6] (generalized speeds [7]) such that the velocity states are the components of the inertial angular velocity when expressed in the body frame ("body rates"). The kinematical differential equations for the orientation can be found in the appendices of [8].

The road arms are mounted in a trailing configuration and are 0.5 meters long with a 0.4 meters radius wheel (wheel plus track). The road arm and wheel system are modeled as a single rigid body with CM at the center of the road wheel. The mass is 136 kg and the mass distribution is that of a uniform disk 0.3 meters thick. The rotational speed of the wheel will be determined by the external track loop and any additional dynamic rotational effects can be incorporated by computing and applying the gyroscopic forces to the road arm. These forces are always out of plane and therefore not essential to the demonstration and are omitted.

The road arms are numbered 1-10 from front to back beginning on the left side of the vehicle and continuing for the last five on the right side. Each road arm is attached by a revolute joint to the hull and described by a relative angle coordinate which is zero when the road arm is in the trailing horizontal configuration. Positive coordinate values indicate vertical travel from zero and the derivatives of the coordinates are used as velocity states.

The suspension forces between the hull and road arm are lumped into an applied moment (Newton · meters) about the joint. Equation (1) gives the relationship for the moment which is in terms of the angle θ (radians), its time derivative, free length $\ell$ (0.5 radians), stiffness $k$ (9000 Nm/rad), damping coefficient $c$ (900 Nm·s/rad), and the jounce bumper displacement $b$ (radians) which is the greater of zero and θ-0.5. The resulting suspension stiffness curve is shown in Figure 2.

$$\mathrm{M}_{\text{suspension}} = k(\theta - \ell) + c\dot{\theta} + k(e^{(40b)} - 1) \qquad (1)$$

Each track loop is 0.4 meters wide and is represented by a lumped rotational degree of freedom. The motion of the loop is an externally specified function such that the vehicle model will perform preprogrammed maneuver. Terrain features encountered are greater than the diameter of the road wheels and their spacing allowing bridging effects of the track to be neglected in the mobility calculation. The track loop is modeled as a prescribed motion of the road wheels and the only feature notably absent is the track tension which can be added as done in [9] but is not an essential feature for the limiting dynamics. The normal and lateral forces from the terrain are applied directly to the road wheel contact point centers but the longitudinal component is properly applied directly to the hull body at a point coincident with the contact point.

The complete rigid body system solution subroutine is automatically generated by a software script [10] which invokes Kane's Method. This solution is a generalized coordinate formulation which ignores constraint forces and is equivalent to using D'Alembert's or Jourdain's principle.

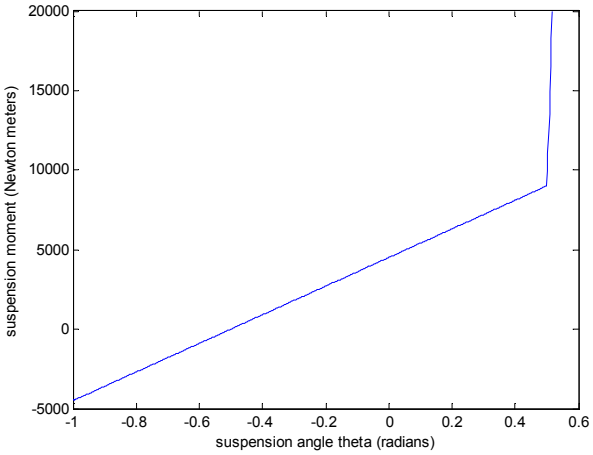


**Figure 2:** Suspension stiffness.

### *Terrain:*

The terrain interface is implemented with a simple spherical contact model where the track and road wheel are assumed to be normal to the terrain at all times. The terrain features have a long wave length such that the surface normal and height can be looked up directly underneath the road wheel center and contact depth determined from the tangent plane. Each road wheel is assumed to have a uniform contact surface area attributed to the track on soft soil 0.6 meters long and 0.4 meters wide.

The soil is modeled as homogeneous dry (11% moisture content) Michigan sandy loam with the Bekker pressure-sinkage relationship of equation (2) [11].

$$\mathrm{p} = \left( \frac{k_c}{b} + k_\phi \right) z^n \tag{2}$$

In equation (2) $p$ is the vertical pressure of a rectangular plate, $z$ is the sinkage, $b$ is the smaller dimension of the plate, $k_c$ is the cohesive modulus of deformation (52.53 kN/m$^{n+1}$), $k_\varphi$ is the frictional modulus of deformation (1127.97 kN/m$^{n+2}$), and $n$ is the exponent of deformation (0.9).

Proper treatment of longitudinal and lateral components requires that the soil be sheared under load to generate reactions. Various steady state slip type models are available most of which are artificially stiff. For the purposes of this model a simple viscous coefficient is applied independently in the longitudinal and lateral directions not to exceed 90% of the normal force.

$$\mathrm{F}_{\mathrm{long}} = -F_{normal} c_{soil} (v_{long} - v_{track}) \tag{3}$$

$$\mathrm{F}_{\mathrm{lat}} = -F_{normal} c_{soil} v_{lat} \tag{4}$$

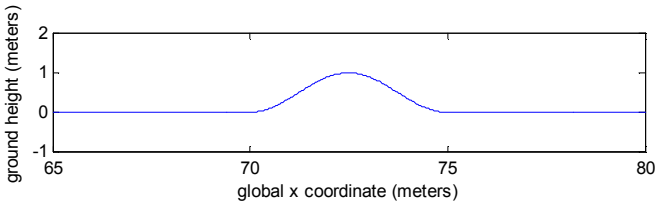


**Figure 3:** Scalable bump obstacle.

The terrain itself is an infinite flat surface with a single scalable height sinusoidal bump obstacle. The sinusoid is defined in the *xz* plane beginning at x = 70 meters with a wave length of 5 meters and is extruded for all values of y. The profile of a 1 meter bump is illustrated in Figure 3.

### *Maneuver:*

During execution of the model the preprogrammed prescribed motions of the sprocket result in a 20.0 second maneuver on the terrain. The maneuver is such that the vehicle begins at rest aligned with the global x direction. It then executes a neutral axis pivot turn to approximately 18 degrees, accelerates to a constant speed 13.5 m/s (30 miles per hour), and drives over the bump at an angle. The left right track speed profile is depicted in Table 1.

## TEMPORAL INTEGRATION

A time integration routine is commonly composed of two components, an integration rule and a step driver. The integration rule describes the method for advancing a given state of a dynamic system to a new state at a discrete time in the future. The step driver manages the task of linking successive discrete instants into the time history which is the desired solution.

| Time (sec) | Left speed (m/s) | Right speed (m/s) | Left Acceleration (m/s$^2$) | Right Acceleration (m/s$^2$) |
|---|---|---|---|---|
| 0 | 0 | 0 | 0 | 0 |
| 3 | 0 | 0 | 0.5 | -0.5 |
| 4 | 0.5 | -0.5 | 0 | 0 |
| 5 | 0.5 | -0.5 | -0.5 | 0.5 |
| 6 | 0 | 0 | 0 | 0 |
| 7 | 0 | 0 | 2.7 | 2.7 |
| 12 | 13.5 | 13.5 | 0 | 0 |

**Table 1:** Track speed profiles.

### *Integration Rules:*

The state space form of the modeled solution of the last section describes a set of first order nonlinear ordinary differential equations (ODEs). There are several excellent texts on the topic of temporal integration routines (such as [12]).

The most common (ODE) integrators belong to the Runge-Kutta family. These solutions are the result of performing a Taylor series expansion about the given state and defining a sequential solution procedure which exactly matches all coefficients to a given order. In the presence of a small step, the truncation error of a single step approximation is many orders of magnitude smaller than the result and the method works very well in practice for many problems. The Runge-Kutta method is succinctly described by equations (5-7) with a Butcher tableau (such as Tables 2 and 3) which collects the coefficients $a_{ij}$, $b_i$, and $c_i$. The $c_i$ are located along the left hand column, $b_i$ along the bottom and the array $a$ in the center.

$$\dot{y} = f(t, y) \tag{5}$$

$$k_i = f\left(t + c_i h, y_n + h\sum_j a_{ij} k_j\right) \tag{6}$$

$$y_{n+1} = y_n + h\sum_i b_i k_i \tag{7}$$

The Butcher tableau for the family of second order solutions (parameterized in α) is given in Table 2 [12] such that a second order rule for advancing the state by a time step $h$ is defined by any choice of α.

The coefficients of a third order rule are given in Table 3 and include an embedded 2nd order solution (α = 1/2) such that both the second and third order estimates are obtained from only two function evaluations [13].

| | |
|---|---|
| 0 | |
| $\alpha$ | $\alpha$ |
| | $1-\frac{1}{2\alpha}$ $\quad$ $\frac{1}{2\alpha}$ |

**Table 2:** Second order Runge-Kutta methods.

| | |
|---|---|
| 0 | |
| $\frac{1}{2}$ | $\frac{1}{2}$ |
| 1 | $-1\quad 2$ |
| | $\frac{1}{6}\quad \frac{2}{3}\quad \frac{1}{6}$ |

**Table 3:** A third order Runge-Kutta method.

The presence of two estimates at varying orders of the same final state enables the construction of an error estimate as the difference between the two state vectors. A "stand alone" third order routine which does not embed a second order estimate should instead use the available degrees of freedom in the selection of the coefficients to further benefit the quality or efficiency of the solution. Often one is able to minimize or eliminate altogether some of the fourth order terms (but the method is still properly considered third order accurate).

The integration rule of Table 3 was implemented as the RK23 routine and used in all simulations. The implementation was then verified to exactly integrate polynomials of orders up to third and second, respectively. The generic integration rule object packages the method for updating the state with a method for estimating the error associated with a single step.

### *Step Drivers:*

The simplest step driver is a fixed step method which merely makes repeated calls to the same rule without any additional logic to control the quality of the solution. These solutions are extremely useful if the system is known to be well behaved and step size criterion is driven by a periodic input or output requirement such as a plot interval, control system, real-time display, and so on. It is useful to note that when implemented with our third order rule, the error associated with each step is readily available but is not used by definition.

Adaptive step integrators control the integration step size dynamically in order to efficiently (quickly) solve the problem subject to a user specified accuracy requirement. For a function evaluation such as given by equation (5), the computational cost of each Runge-Kutta step is assumed to be constant. The efficiency problem then reduces to one of minimizing the total number of steps by taking as big a step as possible without violating the user defined error tolerance.

The common user interface to integration tolerance is scalar values for absolute and relative tolerances. This is in contrast to the indexed array error result which is obtained by the subtraction of the two estimates (second and third order). A vector norm is commonly used to construct a scalar error criterion. In this implementation the maximum individual scalar error is used and only an absolute error value is maintained.

Adaptive step drivers reject and reevaluate any integration step which does not meet the error criterion. The value of the error estimate from the last step (successful or not) and the current step size is used to predict a maximal step size for the interval to be integrated. A conservative safety factor is

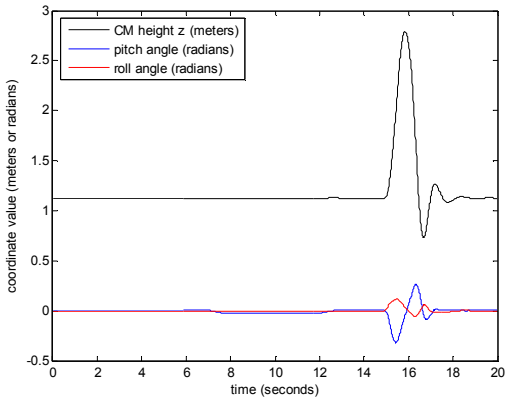


**Figure 4:** Select hull positions and orientations.

generally applied to optimize efficiency by limiting the number of repeated steps.

The RK23 rule was initially matched with this intuitive scaling step driver but an unusually large number of failed integration steps were observed. This was attributed to a misunderstanding in the implementation of relative and absolute errors, but not before a step doubling algorithm was added. The implemented step doubling method simply restricts the amount by which a step can grow or shrink between from successive integration steps (or attempts) and was able to settle the unstable over and under-shooting nature of an earlier step size prediction process.

### *ADAPTIVE AND FIXED STEP SIMULATION*

The fixed step RK3 and adaptive RK23 integrators were applied to the system of equations which describe the tracked vehicle example problem with a terrain consisting of a 1.0 meter bump. The fixed step integrator is set to evaluate the problem at 200Hz, 500Hz, and 1 kHz (step sizes of $5\text{x}10^{-3}$, $2\text{x}10^{-3}$, and $1\text{x}10^{-3}$ seconds). The adaptive step method is assigned an absolute error tolerance of $1\text{x}10^{-3}$ and output for all simulations is collected at 100Hz (0.01 second time intervals).

The simulations demonstrate the expected result of excellent agreement among the four simulations in the recorded positions and velocities of the chassis and road arms. In the vicinity of the 1.0 meter bump event the loads diverge from the trusted prediction of the adaptive step driver solution. Figures 4 through 7 show the overall hull CM motion in the vertical (*z*) direction as well as the pitch and roll coordinates using the adaptive step integrator. Figures 5 and 7 show detailed comparisons across the adaptive step and various fixed step solutions, and the solutions are drawn on top of each other and observed to be indistinguishable.

Figures 8 and 9 demonstrate a similar performance comparison with road arm motions relative to the chassis.

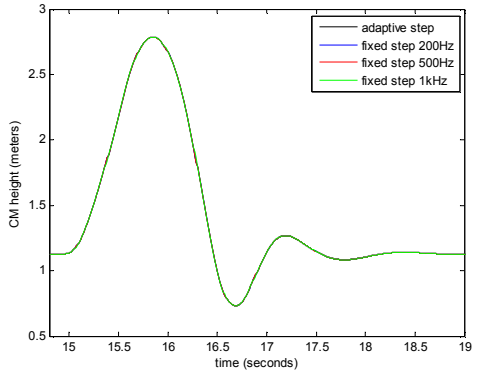


**Figure 5:** Hull CM vertical position.

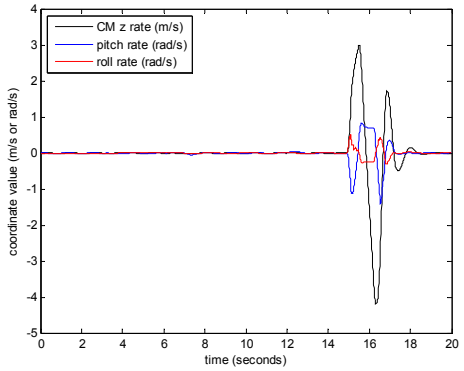


**Figure 6:** Select hull rate plots.

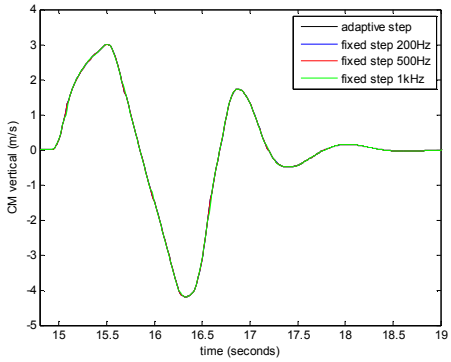


**Figure 7:** Hull vertical rate.

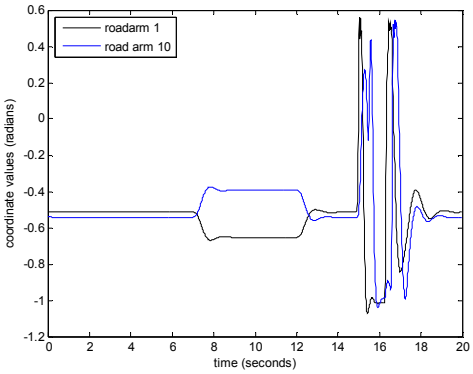


**Figure 8:** Select road arm orientations.

The applied moment between the road arms and hull are shown in Figures 10, 11, and 12 and demonstrate the nature of the fixed step integrator for this problem. Specifically, the peak load is predicted as -121 kNm, -109 kNm, or -125 kNm with decreasing step size. The accepted result obtained from the adaptive step integration is -131 kNm. To capture the peak loads it was necessary in Figures 10 through 12 to collect the output at the completion of every integration step.

The accuracy performance of the adaptive step integrator is shown in Figure 13. Highly accurate values are obtained relative to the $1 \times 10^{-3}$ error because the maximum step size is limited to 0.01 seconds for output purposes. Figure 14 gives the step size requirements of the adaptive step integrator throughout the simulation and succinctly characterizes the nature of agreement between all results. The constant step sizes of the three fixed step solutions appear as horizontal lines to clearly illustrate that the fixed step solutions encounter problem areas and will not maintain accuracy.

### *A Hybrid Method*

As mentioned previously, failures of the fixed step routine to predict the applied loads can be readily detected through examination of the embedded RK23 error check. This is a common feature in adaptive step algorithms and many other

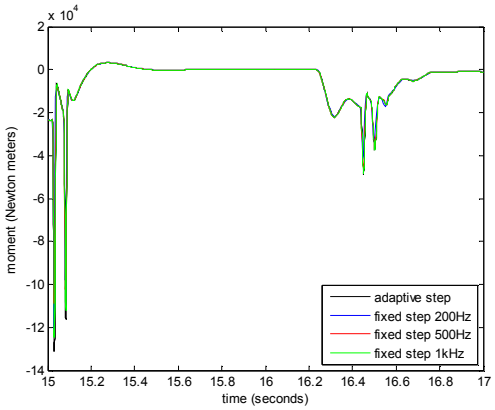


**Figure 11:** Road arm 1 moments over bump.

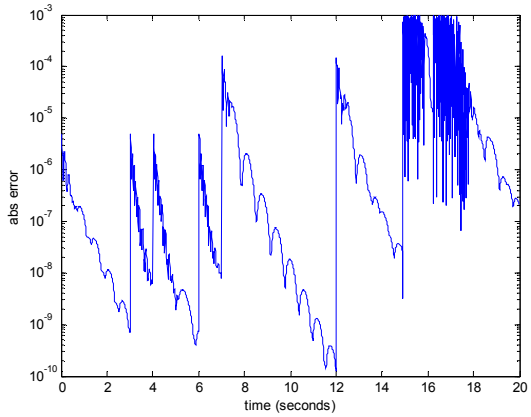


**Figure 13:** Adaptive step error.

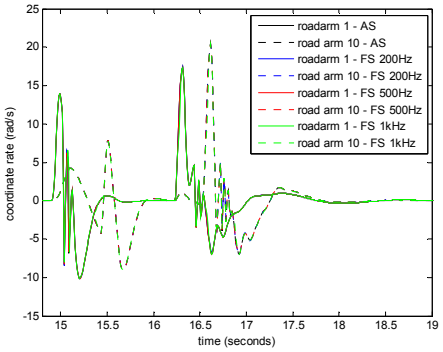


**Figure 9:** Select road arm rates.

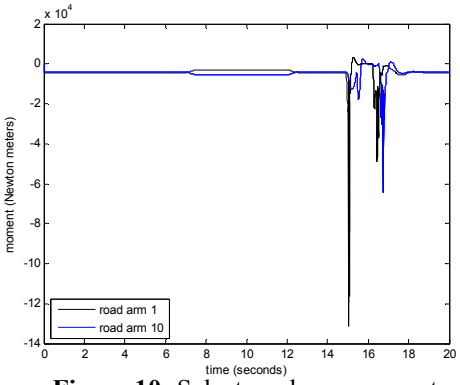


**Figure 10:** Select road arm moments

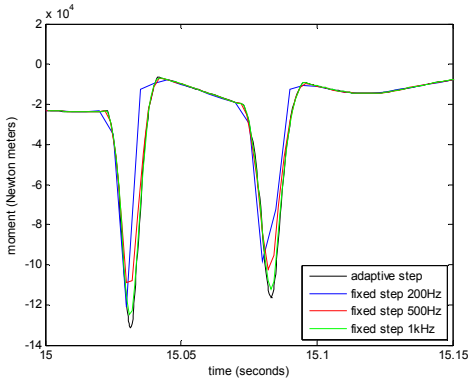


**Figure 12:** Road arm 1 moments near 15 seconds.

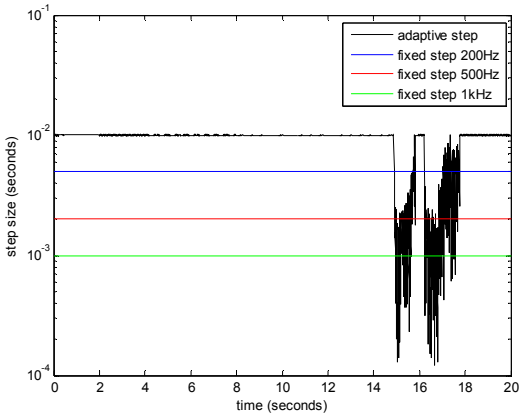


**Figure 14:** Adaptive step size.

adaptive step embedded pairs are readily available in the literature for this and other orders of accuracy. The computational cost of the embedded error estimate is extremely low and although an exhaustive literature has not been conducted, it is reasonable to expect that some real-time systems have already applied this type of solution to alert users of instabilities or trigger a stable "safe mode" solution to carry the vehicle to the other side of a series of stiff time steps. This same identification should be present in loads data generated from fixed step simulation.

From this point analysts can extract the initial conditions for invalidated fixed integration steps and re-run them off-line with an adaptive routine after the fact, and obtain accurate loads. This would work provided stiff steps do not occur in rapid succession such that artificial transient behaviors can damp-out and not unduly influence the initial conditions for another off-line evaluation.

Unfortunately, Figure 14 has already demonstrated this to be many steps for this simple singular event, and for a real durability road, the data would simply tell the user to re-evaluate the entire course! Furthermore, it is not demonstrated in these simulations, but loss of stability after a stiff event is also a principal concern and there is no reason to assume that what comes out "the other side" of a very poor integration step is a valid approximation for the initial state of the next. An alternate and trusted solution is required in the stiff regions of the response.

A second observation is that the integration error routine can also identify the generalized coordinate or coordinates (degrees of freedom) which are causing integration to fail. The identified degrees of freedom are appropriately thought of as having encountered stiffness in excess of the ability and/or desire to proceed as a continuous component of the time response. From a practical perspective, elements which are significantly stiffer than the rest of the problem are appropriately modeled as rigid, and the analog for stiff reactions is impact and associated impulsive forces. This method is markedly different than that of traditional contact/impact problems where the impulsive event is a function of geometry. This modeling technique suggests application to many non-conventional impulsive events which will be summarized later.

For the tracked vehicle model, the trusted impact impulsive solution is a multibody momentum method. A standard generalized momentum solution as described in any applied or analytical dynamics text (such as [6] or [7]) is applied as shown in equations (8) and (9).

$$\sum_i \left( m_i v_i^{+} \cdot \frac{\partial v_i}{\partial u_r} + I_i \cdot \omega_i^{+} \cdot \frac{\partial \omega_i}{\partial u_r} \right) - F_c \Delta t \cdot \frac{\partial v_c}{\partial u_r} = \sum_i \left( m_i v_i^{-} \cdot \frac{\partial v_i}{\partial u_r} + I_i \cdot \omega_i^{-} \cdot \frac{\partial \omega_i}{\partial u_r} \right) \tag{8}$$

$$v_c^{+} \cdot \hat{n} = -\varepsilon v_c^{-} \cdot \hat{n} \tag{9}$$

In equations (8) and (9) the mass $m$, central inertia dyadic $I$, velocities $v_i$ and angular velocity $\omega_i$ vectors of each body $i$ have the usual meanings. The $F_c$ and $\Delta t$ are the force of contact and the time interval, assuming for the moment that $\Delta t$ is zero the $F_c$ is infinite and the product is a finite impulse. The superscripts + and - represent the instant before and after the impulse is applied. Equation (8) then represents $n$ total equations in the unknowns $u_r$ which are generalized speeds (quasi-coordinate velocities) and equal to the coordinate derivatives except for those describing the orientation and angular velocity relationship of the hull body. The $n$ equations contain numerous solutions and require further constraint which is applied from the coefficient of restitution (CoR) relationship of equation (9). The vector $\hat{n}$ is the contact unit normal direction and ε is the CoR. A CoR of 1.0 was used for all cases as the system posses enough dissipation to account for the momentary omission.

Equations (8) and (9) may be put in matrix form by stacking the two relations and extracting the unknowns ($u_r$ and $F_c\Delta t$) and collecting the coefficients in matrix form. This was largely accomplished within software [10] and code generated for an additional solver subroutine.

For the purposes of simulation, a new hybrid step driver was created such that individual fixed steps which violate the error criterion are identified. When violations are detected, the routine undoes the step solution (in exactly the same way the adaptive step routine does). Then the impulsive solution is called, the initial states updated, and the step recomputed. This type of solution is slightly more than twice as computationally intensive as the fixed step but is deterministic.

In practice the applied impulse can cause additional degrees of freedom to go unstable during the same time step, so several iterations may be required (but limited by the system DoF. Furthermore, the stiff interactions with the round and the jounce bumper actually caused the solution to enter an infinite loop. To remedy this issue, the impulsive solve was expanded to a finite time covering one time step and the CoR relationship programmed as a specified constant acceleration throughout the step. Because the integrator is third order, the unstable degrees of freedom are always integrated exactly, with zero error over the prescribed time step.

The hybrid impulsive solution method characterizes the loads in terms of the reliable continuous values plus a set of impulses obtained from the solution of equation (9). Here again the initial conditions for the impulses can be recorded and continuous time histories reconstructed, or significant time savings can be made in several ways.

First, one can assume that the system does not move much during the stiff event and integrate the system rapidly with many static assumptions (notably that the mass matrix remains constant). Another choice is to integrate the event locally with a reduced number of degrees of freedom. Lastly, one can construct a surface of peak load versus configuration and impulse magnitude and evaluate only a small fraction of the actual impulses, interpolating the rest.

## RESULTS

The hybrid impulsive scheme was implemented for the same fixed step sizes as studied earlier (200 Hz, 500 Hz, and 1 kHz). Application to the earlier example system produces Figures 15 through 20. The reference trajectory is again taken as the adaptive step (AS) solution and shown with each result.

Figures 15 through 19 showcase the ability of the hybrid step routine to mimic the overall behavior of the vehicle motions. There is a recognizable difference in the trajectories, particularly at the velocity level associated with the abrupt reversal of velocities (Figure 19). However, provided that trajectory is stable and does not represent a significant difference in the system energy, such solutions are properly considered superior to uncontrolled and potentially unstable fixed steps.

The aim of the hybrid step was to generate more accurate loads and this is demonstrated in Figure 20. In this case the loads were obtained by integrating the impulse event from the prior initial conditions with a constant mass matrix. The present state of the post processed solution contains all internal and external forces and moments, further approximation is the subject of future work. The complete load history is then assembled by replacing the forces during the impulse event with the peak result from the fully integrated time history.

The results demonstrate construction of consistent and stable load time histories across 200 Hz to 1kHz.

## DISCUSSION

The results describe a new loads reporting format which isolates the peak loads occurring in the stiffest part of the response from the smoother parts of the trajectory and applied forces/moments. The method takes advantage of the controlled and dissipative nature of vehicle dynamics to create an alternate description of vehicle road loads as a series of impulsive events which runs quickly.

Use of impulses can also be observed to decouple the design problem of jounce bumper (or other stiff components) from the vehicle dynamics which involves lengthy computations. In this example the jounce bumper may be redesigned to soften the peak loads without re-running a vehicle dynamic simulation.

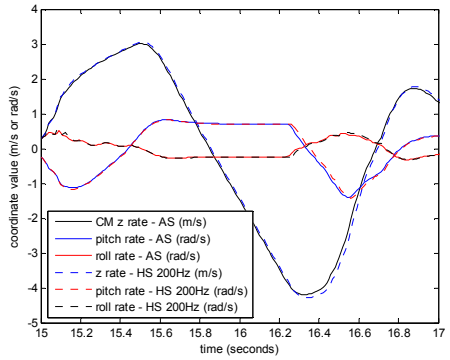


**Figure 15:** Hybrid step hull rates comparison at 200Hz.

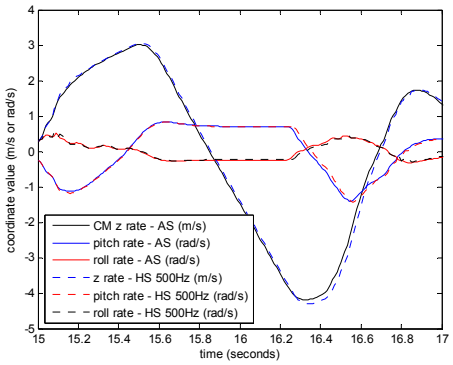


**Figure 16:** Hybrid step hull rates comparison at 500Hz.

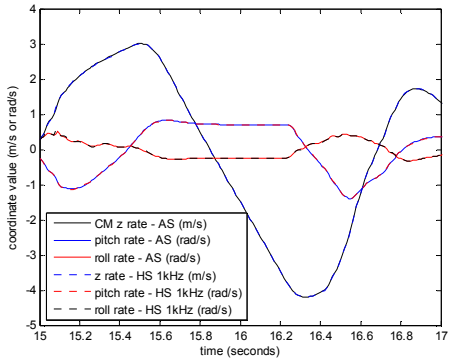


**Figure 17:** Hybrid step hull rates comparison at 1kHz.

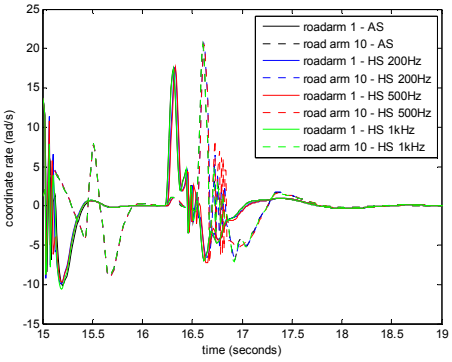


**Figure 18:** Select road arm rates comparison over bump.

Stiffness need not come from jounce bumpers, rebound bumpers, or predictable geometric configurations with this method. The key contribution is the ability to identify stiffness dynamically and apply the impulsive approximation based on a numerical rather than geometric requirement. This enables designs to be evaluated automatically, with dynamically changing masses and interaction force models without user intervention. In contrast to geometric based contact/impact solutions this method automatically allows the continuous simulation of smooth controlled contacts without automatically calling the impact solution. It readily adapts to variable ride height designs and can be applied to control laws and other potentially stiff actions.

The implementation of the solution as a finite time impulse is most appropriately described as prescribed objective modeling. In the case of the jounce bumper or the ground, the objective is to fully reverse the velocity of the road arm. Associating similar objectives with other force elements such as controllers and other aspects of machine motions is an aspect of simulation often ignored by analysts and requires tighter integration with design intent.

With this method it is most appropriate to identify the force contributions which are stiff rather than the degree of freedom. Significant clues can come from analysis of the degrees of freedom which are impacted, and from this perspective the tracked vehicle was an ideal starting point for analysis because the design serves to limit the selection of stiff forces. In future applications to this and other systems it is recommended that auxiliary states which are the applied forces be tracked/integrated so that the accuracy of the polynomial representation can be assessed directly and stiffness attributed immediately to the correct source.

These and other observations are the subject of future work.

## SUMMARY

A new hybrid impulsive solution for off-road vehicle dynamics has been described and demonstrated in a limited tracked vehicle simulation environment. The hybrid solution describes a new loads reporting format which isolates the peak loads occurring in the stiffest part of the response from the smoother parts of the trajectory and applied forces/moments. The solution method is shown to be consistent with the first order accuracy and greater detail is demonstrated for typical tracked vehicle suspensions. Enhanced detail in all cases is limited by the exact constraints which replace bushings in real-time environments and cannot distribute loads to kinematically redundant attachments. In general the method provides appropriate support for both conceptual design optimization (travel, stiffness, and control) and developmental tuning relative to a baseline loads model. Several avenues for future research associated with the decoupling have also been exposed.

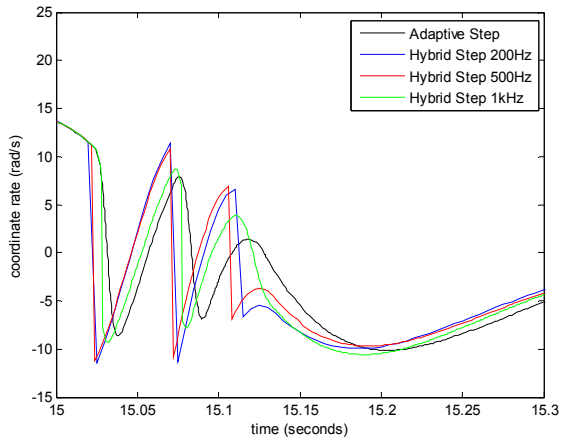


**Figure 19:** Road arm 1 rates comparison near 15 seconds.

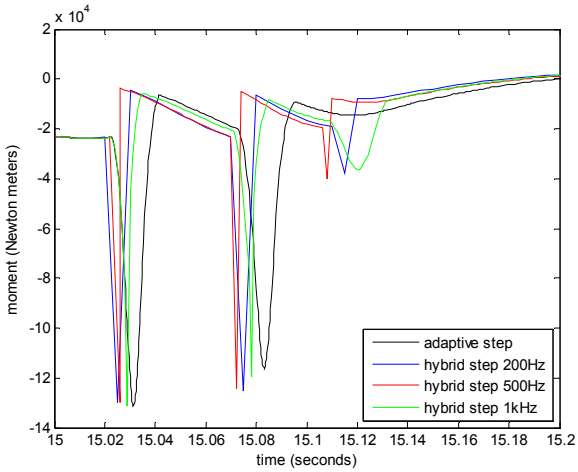


**Figure 20:** Road arm 1 moments near 15 seconds.

## REFERENCES

[1] ADAMS, MSC Software, www.mscsoftware.com.

[2] Berzeri, M. et al., "A New Tire Model for Road Loads Simulation: Full Vehicle Validation," SAE Paper No. 2004-01-1579, SAE 2004 World Congress & Exposition, Detroit, Michigan, 2004.

[3] Masini, C., and Yang, X., "Influence of Shock Absorber Model Fidelity on the Prediction of Vehicle Half Round Performance," Ground Vehicle Systems Engineering and Technology Symposium, Dearborn, Michigan, 2010.

[4] Jayakumar, P., Alanoly, J., and Johnson, R., "Three-Link Leaf-Spring Model for Road Loads," SAE Paper No. 2005-01-0625, SAE 2005 World Congress & Exposition, Detroit, Michigan, 2005.

[5] Romano, R., “Realtime Driving Simulation Using A Modular Modeling Methodology,” SAE Technical Paper Series No. 2000-01-1297, March, 2000.

[6] Rosenberg, R.M., "Analytical Dynamics of Discrete Systems," Plenum Press, New York, 1977.

[7] T.R. Kane and D.A. Levinson, "Dynamics: Theory and Applications," McGraw-Hill, New York, 1985.

[8] Kane T.R., Likins P.W., and Levinson D.A., “Spacecraft Dynamics,” McGraw-Hill, New York, 1983.

[9] McCullough, M.K., and Haug, E.J., "Dynamics of High Mobility Tracked Vehicles," ASME, Journal of Mechanisms Transmissions, and Automation in Design, Vol.108, pp.189-196, 1986.

[10] Schaechter, D.B., Levinson, D.A., and Kane, T.R., "Autolev User's Manual," OnLine Dynamics Inc., Sunnyvale, CA, 1989.

[11] Wong, J., "Theory of Ground Vehicles," John Wiley & Sons Inc., New York, 2nd ed., 1993.

[12] Ascher, U.M., Petzold, L.R., “Computer Methods for Ordinary Differential Equations and Differential-Algebraic Equations,” Society for Industrial and Applied Mathematics (SIAM), Philadelphia, 1998.

[13] Compare, M., “Octave ode23,” http://octave.sourceforge.net/, 2001.